Battery-free UHF-RFID Sensors based SLAM for In-Pipe Robot Perception

Amal Gunatilake, *Member, IEEE*, Sarath Kodagoda, *Member, IEEE*, and Karthick Thiyagarajan, *Member, IEEE*

***Abstract*— Water utilities across the globe are concerned with the inspection and replacement of buried metallic water pipes due to corrosion-related structural damages. Internal pipe linings are commonly used as a renewal method to improve structural strength as they are regarded to be a less expensive alternative to costly and time-consuming pipe replacements. However, linings are also prone to failure as well. Therefore, water authorities regularly monitor lining performance, where defect evolution over a long period of time is an important parameter to note. It requires an accurate in-pipe robot localization technology. In this article, we propose a novel method for in-pipe robot localization and tag mapping that uses battery-free UHF-RFID sensor wireless signals. It utilizes a signal mapping approach in combination with a tailored pose-graph simultaneous localization and mapping algorithm. Evaluation results of a field-extracted pipe sample from Sydney Water's distribution network show the proposed approach is capable of localizing the robot within 2.5cm accuracy in a 50m equivalent pipe with an unknown UHF-RFID distribution. The proposed approach outperformed other reported similar work in the literature.**

***Index Terms*— Sensor applications, battery-free sensors, infrastructure sensing, UHF-RFID sensors, pipe sensing, pipe robotics, infrastructure robotics, robot localization, robot perception, field robotics, SLAM.**

I. Introduction

Many cities around the world experience greater incidences of water and wastewater pipe leaks and breaks, both of which cause significant economic, social, and environmental damage [1]–[3]. This is exacerbated by ageing assets and hence timely monitoring of them is essential for identifying faults and determining the most effective ways of renewal [4]. CIPP (Cured in Place Pipe) [5] or spray techniques [6] are widely utilized in the "lining" process, which is a popular form of renewal. Despite the fact that a variety of robotic technologies are available for the condition assessment of host pipes [7], [8], they do not provide critical information about the quality of the liners and their long-term performance. Common defects of liners are folds, bulges, wrinkles, dimples, thickness variations, etc. [9]–[12]. Post-application condition assessment of liners improves the confidence in the application whereas long-term monitoring can identify defects that can potentially lead to pipe failures. Currently, it is accomplished through the use of CCTV technology, either based on subjective visual analysis or through the experience of an operator.

Laser profiling and ultrasound technology are two examples of emerging technologies that can be used to monitor the quality of water pipe linings. The improved solution for laser profiling that we proposed in our previous work [12], [13] has the capability of taking measurements with millimeter-level accuracy. When it comes to reconstruction in the radial direction, the solution is effective and efficient. However, it has limitations as a result of longitudinal errors accumulating over time and distance when encoder-based localization is employed. This is particularly unacceptable in the context of long-term defect monitoring, where it is necessary to correlate a specific defect across multiple deployments occurring at different time intervals. Flying and floating robots are not meant for encoder-based localization. Due to the inherent visual feature changes caused by the application of liners, emerging corrosion patches, and possible alien buildups, popular outdoor localization methods such as visual SLAM become infeasible in underground pipeline infrastructure. This necessitates the development

This work was supported by the University of Technology Sydney (UTS) through the Faculty of Engineering and Information Technology (FEIT) Tech Lab Blue Sky Research Grant. All the authors are with the iPipes Lab, UTS Robotics Institute, Faculty of Engineering and Information Technology, University of Technology Sydney, Sydney, New South Wales, 2007, Australia (e-mail: Amal.Gunatilake@uts.edu.au; Sarath.Kodagoda@uts.edu.au; Karthick.Thiyagarajan@uts.edu.au). Corresponding Author: Sarath Kodagoda

of an alternative and more efficient contact-less localization method.

There are many different wireless technologies and algorithms are being researched for use in indoor and outdoor environments [14]–[19]. The use of radio-frequency identification (RFID) localization technology has produced reasonable localization results for indoor and outdoor environments [20]–[25]. Therefore, we attempted to use RFID in in-pipe environments. They also have other benefits, such as cost-effectiveness and the ability to measure various environmental conditions inside pipelines, such as temperature, moisture, and acidity levels, by embedding them as liner embedded sensing technologies [26]–[28]. Temperature is a good proxy for liner curing, moisture can indicate leaks, and acidity level is a corrosion indication. As a versatile sensor, RFID has numerous advantages in in-pipe applications. Unfortunately, there hasn't been much research on subsurface pipeline robot localization utilizing RFID sensors as of yet. This could be owing to the application's intrinsic complexities. Unlike RFID localization in outdoor or indoor applications, the highest peak of signal intensity is not always referring to the most likely location of the RFID tag [29], [30]. The pipe surface behaves like a waveguide causing the signal inside to bounce leading to various peaks and ripple effects in the signal strength [31], [32]. Furthermore, commercial off-the-shelf (COTS) RFID readers offer erratic measurements, only capable of accurately localizing the RFID tag within a square meter area [33], making the process difficult and unique.

The Gaussian process combined particle filter localization methodology using UHF-RFID signals has been proposed in our previous research [31], [32], [34], and it takes advantage of both Received Signal Strength Indicator (RSSI) and Phase data values to improve accuracy. It works well with known RFID distribution maps (RFID tag locations are known), and it has millimetre-level accuracy when using known RFID distribution maps. In practice, however, the premise of the availability of an accurate RFID distribution map, to begin with, is less practical than it appears in theory. As a result, we present in this study an RFID localization system that employs a signal mapping approach in combination with a customized simultaneous localization and mapping algorithm which does not require the RFID distribution map to be known as a priory. The main contributions of this paper are briefly elucidated as follows:

1) Development of an in-pipe robotic prototype for simultaneous localization and mapping with a custom measurement model using dual-antenna UHF-RFID RSSI signal cross-correlation.
2) The system can be deployed from any location within a pipe to travel in either direction while building RFID tags location maps and localizing the robot simultaneously with approximately 2.5 cm accuracy.
3) The system works independently without the aid of any other odometry system and requires only a training data set acquired in a laboratory pipe sample. It does not require any specific field calibration.
4) Demonstration of the superiority of the proposed localization by comparing it with industry standards and relevant localization approaches reported in the literature.

The rest of this article is structured as follows: Section II formulates the SLAM problem, while Section III formulates the pose graph optimization and UHF-RFID signal mapping. Section IV describes the RSSI cross-correlation matching and Section V presents the experimental results. Section VI concludes the article by summarizing the key outcomes while briefing the intended future work.

II. Simultaneous Localization and Mapping

The conventional Pose-Graph optimization problem solver [35]–[37] has been used to localize the robot inside the pipeline with respect to the UHF-RFID measurements received from the sensor model. The motion model of the robot's movement along the pipe can be defined as in (1):

$$x_t^r = g\left(u_t, x_{t-1}^r\right) + \omega_t \tag{1}$$

where x_t^r is the one dimensional position of the robot along the axis of the pipeline at time instance t, u_t is the input given to the robot at time instance t, g is a nonlinear function for state transitions, and ω_t is random Gaussian distributed noise where $\omega_t \sim N(0, R_t)$.

Following that, the UHF-RFID (landmark) measurement model of the robot can be defined as in (2):

$$z_t^i = h\left(x_t^r, x^i\right) + \upsilon_t \tag{2}$$

where z_t^i is the UHF-RFID measurement from the UHF-RFID tag landmark i at the time t, x^i is the UHF-RFID RSSI measurement of the landmark i, h is a nonlinear measurement model, and υ_t is random Gaussian distributed noise for measurement where $\upsilon_t \sim N(0, Q_t)$. The robot only senses UHF-RFID tags that are closer to the robot. Therefore, for some time indices t, there can be no measurements.

The conventional pose-graph optimization problem [35] cost function can be defined as in (3):

$$\begin{aligned} J &= x_0^{rT} \Omega_0 x_0 \\ &+ \sum_t^\tau \left(x_t^r - g\left(u_t, x_{t-1}^r\right)\right)^T R_t^{-1} \left(x_t^r - g\left(u_t, x_{t-1}^r\right)\right) \\ &+ \sum_t^\tau \sum_i^I \left(z_t^i - h\left(x_t^r, x^i\right)\right)^T Q_t^{-1} \left(z_t^i - h\left(x_t^r, x^i\right)\right) \end{aligned} \tag{3}$$

where x_0 is the initial state of the robot, R_t^{-1} is the covariance of motion noise and Q_t^{-1} is the covariance of measurement noise. Signal cross-correlation is used to estimate the distance from the robot to an RFID tag. The uncertainty values returned from the signal cross-correlation mapping are used as the covariance of Q. Motion model-related uncertainty was tuned based on the performance. Ω_0^{-1} is an information matrix. In this matrix, the off-diagonal elements are all zero other than between any two consecutive robot poses or any element between a

map feature and a robot pose, if a map feature was observed by the robot at that time instant. Entries relating to pair of features are zero. τ is the number of time steps for the robot, and I is the number of features. The defined problem in (3) can be solved as an optimization problem using (4).

$$\mathbf{x}^* = \underset{\mathbf{x}}{argmin}\ J(\mathbf{x}) \tag{4}$$

where $\mathbf{x}$ is given as

$$\mathbf{x} = \begin{bmatrix} \mathbf{x}^r_{0:\tau} \\ \mathbf{x}^{0:I} \end{bmatrix} \tag{5}$$

Using numerical methods, this optimization problem has been solved iteratively to compute the gradient.

III. Pose Graph Optimization with RFID Signal Mapping

The robot trajectory path estimations and the UHF-RFID sensor (landmark) location estimations need to be simultaneously optimized. Therefore, UHF-RFID RSSI signal measurements need to be incorporated into the optimization problem. This has been achieved by incorporating the RSSI signal s_t into the pose-graph optimization problem in equation (3) with an additional cost function ϕ that denotes the inconsistency of the signal measurements along the pipe traverse. The updated equation is defined as in (6):

$$\begin{aligned} J = {} & x_0^{rT}\Omega_0 x_0 \\ & + \sum_t^{\tau} \left(x_t^r - g\left(u_t, x_{t-1}^r\right)\right)^T R_t^{-1} \left(x_t^r - g\left(u_t, x_{t-1}^r\right)\right) \\ & + \sum_t^{\tau}\sum_i^{I} \left(z_t^i - h\left(x_t^r, x^i\right)\right)^T Q_t^{-1} \left(z_t^i - h\left(x_t^r, x^i\right)\right) \\ & + \sum_t^{\tau} \phi\left(t, \mathbf{x}^r_{0:\tau}, \mathbf{s}_{0:\tau}\right)^T P_t^{-1} \phi\left(t, \mathbf{x}^r_{0:\tau}, \mathbf{s}_{0:\tau}\right) \end{aligned} \tag{6}$$

where $\mathbf{x}^r_{0:\tau}$ is the robot positions along the pipe, $\mathbf{s}_{0:\tau}$ is the RFID signal measurements along the pipe, and P_t is the covariance of the measurement model noise. Function ϕ can be defined as in (7):

$$\phi\left(t, \mathbf{x}^r_{0:\tau}, \mathbf{s}_{0:\tau}\right) = y\left(t, \mathbf{x}^r_{0:\tau}, \mathbf{s}_{0:\tau}\right) - f\left(t, \mathbf{x}^r_{0:\tau}, \mathbf{s}_{0:\tau}\right) \tag{7}$$

where y is a function that calculates the distance between matching points of the signal $\mathbf{s}$, and f is a function that calculates the distance between matching points in the estimations of $\mathbf{x}$.

IV. RSSI Signal Cross-Correlation Matching

Let $\left[\mathbf{x}^r_{p1}, \mathbf{s}_{p1}\right]$ be the training data collected from the robot at the initial deployment in the lab pipe environment, and $\left[\mathbf{x}^r_{p2}, \mathbf{s}_{p2}\right]$ be the data received from the robot during the localization task. Before performing cross-correlation, the equal number of comparison data points are generated with data interpolation. Let the new sets of points be $\left[\mathbf{x}^r_{q1}, \mathbf{s}_{q1}\right]$, $\left[\mathbf{x}^r_{q2}, \mathbf{s}_{q2}\right]$ where $\left[\mathbf{x}^r_1, \mathbf{s}_1\right]$ and $\left[\mathbf{x}^r_2, \mathbf{s}_2\right]$ be the subsets of points. the normalized cross-correlation coefficient γ between the two sets of data can be calculated using (8).

$$\gamma = \frac{\sum_x \left(\mathbf{s}_1(x) - \overline{s_1}\right)\left(\mathbf{s}_2(x) - \overline{s_2}\right)}{\sqrt{\sum_x \left(\mathbf{s}_1(x) - \overline{s_1}\right)^2 \sum_x \left(\mathbf{s}_2(x) - \overline{s_2}\right)^2}} \tag{8}$$

For each window, when the signals are aligned properly, the difference (Euclidean distance) between the signals is calculated using (9) as a confidence η parameter for later use in the optimization.

$$\eta = \frac{1}{\sum_x \left(\mathbf{s}_1(x) - \mathbf{s}_2(x)\right)^2} \tag{9}$$

The final confidence parameter ϵ is calculated using the results of both (8) and (9) as in (10).

$$\epsilon = ((1+\gamma)\eta)^2 \tag{10}$$

where best matching poses can be filtered by setting a threshold value to the calculated ϵ. The corresponding poses that represent the filters $\mathbf{s}_1$ and $\mathbf{s}_2$ are added to the cost function (7) where measured distance and expected distance given by (11) and (12).

$$y_t = 0 \tag{11}$$

$$f_t = \widetilde{x_1^r} - \widetilde{x_2^r} \tag{12}$$

where $\widetilde{x_1^r}$ and $\widetilde{x_2^r}$ are the corresponding poses when $\mathbf{s}_1$ and $\mathbf{s}_2$ signals are matching signals. The signal mapping process depends on the many numbers of poses in $\mathbf{x}^r_{0:T}$, which can be a heavy computational cost. Therefore, the signal noise covariance P_t has been used as inversely proportional to $(\gamma \times \eta)$, so that stronger matches effectively weight the cost function in (3).

V. Experiments & Results

A. Development of an In-pipe Robotic Prototype for SLAM

The developed in-pipe robotic system and two-layer system architecture utilized are shown in Fig. 1 and Fig. 2.

1) Hardware Developments: The RFID unit mounted on top of the robot has been built using commercially available off-the-shelf (COTS) components. Thingmagic M6e Micro-LTE UHF 2 port RFID reader module with embedded developer kit has been used to implement the proposed system. Two 915MHz General Purpose Panel RF Antennas in the 902MHz to 928MHz range with 5.5dBi gain were used as the receiver antennas. The two antennas are directed in the travel direction of the robot. It can be analogously similar to a stereo camera system. UHF-RFID Tag type A and B discussed in [31] has been used to conduct experiments. An industry standard infrared laser distance sensor with 80m range, and 1mm accuracy has been used as the robot's location ground truth. When the robot is moving forward, the distance to the object is decreasing and hence the laser-based distance to the object. Even though laser localization is quite accurate, in order to perform laser-based localization, the pipe needs to be straight, so that the

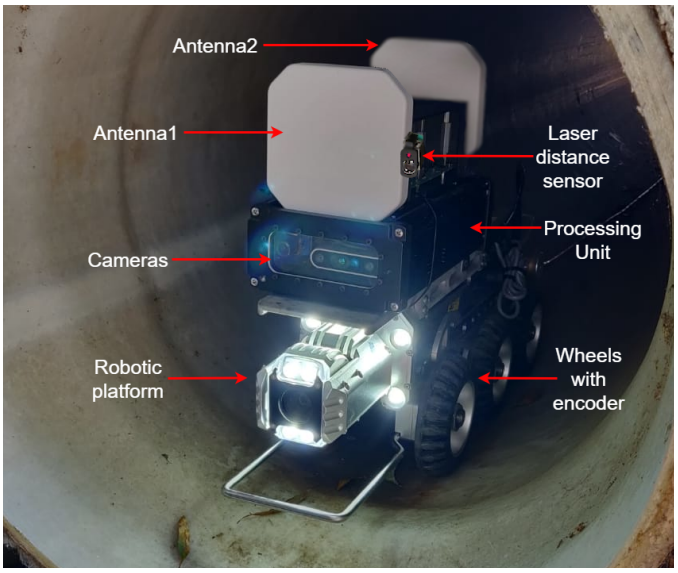

Fig. 1: An in-pipe mobile robot integrated with two UHF-RFID reader antenna.

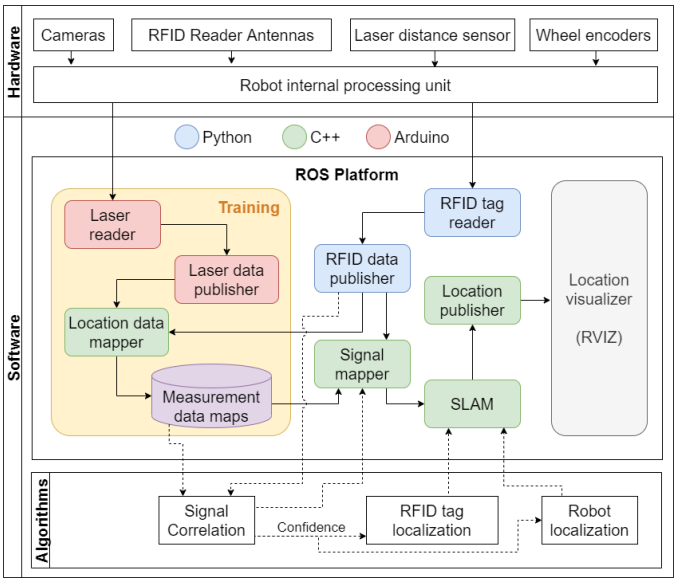

Fig. 2: In-pipe robot system architecture.

laser pointer can be focused from the robot to an object at the end of the pipe during the whole journey. Underground pipelines are not perfectly straight, and the robot can have pan and tilt movements causing the laser pointer to incident on pipe surfaces rather than the end of the pipe object causing localization errors. Although the laser system is cheap, it is not practical to use it as a general localization method in this application. In our experiments, the laser localization is used only for a shorter pipe length to create the measurement model and finally compare the accuracy of localization by using it as the ground truth. In order to compare the performance with the standard wheel encoder-based odometry, a calibrated, industry-standard 2400 pulses per revolution rotary encoder has been used to record the odometry by attaching it to the robot wheel. The Jetson Nano Developer kit board with a Quad-core ARM 1.43 GHz CPU, and 4 GB 64-bit LPDDR4 RAM was used as the central processing unit to run the implemented system. The whole hardware system was assembled inside an enclosure and mounted on the robotic platform, miniPIRO as shown in Fig. 1.

2) Software Developments: The software components were implemented with the Robot Operating System (ROS) framework to gain the flexibility to modularize each component and to gain cross-language software support. Each individual component has been implemented as ROS node to communicate with each other effectively. UHF-RFID-related components are implemented in Python as they are supported by the open source Python Mercury API library. To gain more structure and flexibility to implement the algorithms, the core integration has been implemented as C++ components. The laser distance sensor that tracks the odometry of the robot has been implemented with Arduino components. As the diagram elaborates, the UHF-RFID component receives the RSSI and Phase data signals from the robot and publishes the data to the receiving components. In the training phase, the location mapper will combine the data with robot odometry data that is received from the laser data publisher node. The collected data will be stored as measurement data maps for later use in signal mapping. In the localization phase, the data received from the robot is mapped with the measurement model using the signal correlation algorithm. Based on the generated confidence value, the probabilities of robot location and tag locations are calculated within the SLAM algorithm for each UHF-RFID tag signal. Finally, using these calculated values, the highest probability of the robot localization and UHF-RFID tag locations are published to the location publisher node, which is displayed in RVIZ like location visualizer systems.

B. Data collection, Data Modeling and Signal Mapping

Tethered heavy crawler robots are not preferred to be deployed in pipes with corners and bends as they tend to tangle or tear the tether. In practice, most of the water pipe inspections of medium-sized pipes (300mm – 900mm diameter pipes) are carried out over shorter distances (less than 500m) and they are reasonably straight. In medium-sized non-traversable sewer pipes (900mm - 1500mm diameter), manhole to manhole deployments is generally carried out, ranging from 100 – 300 meters. In Sydney, they are generally straight pipe sections, which led us to simplify the localization problem. However, in pipe environments with possible bends, this system can be modified with an IMU sensor and/or prior knowledge of network drawings to deal with the changes in orientation.

Data for training the measurement model was collected by placing UHF-RFID tags in the middle of the side wall of 5 meters long, 600-millimeter diameter pipe section. According to our previous studies [32] all tags perform similarly, and RFID tags did not interfere with each other. The closer the RFIDs were packed, the more the measurements were

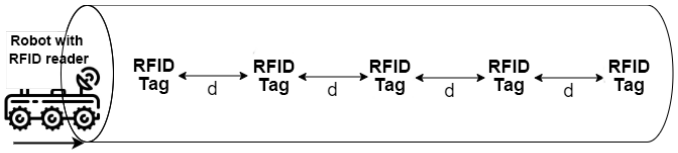

Fig. 3: Testbed setup for data collection and in-pipe robot localization validation.

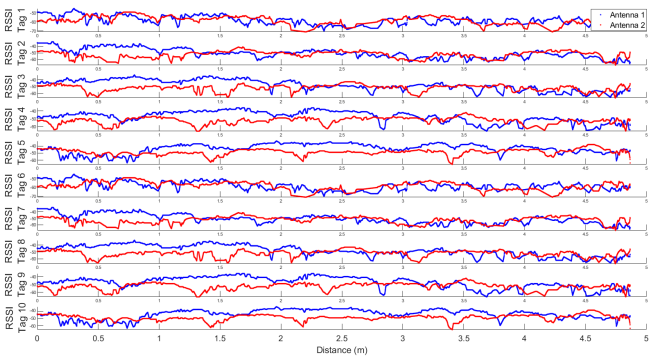

Fig. 4: First 10 segments of the measurement model. RSSI (dB) for each UHF-RFID sensor tag is plotted against the robot travel distance (m).

received. Having more measurements in the training model will help with the accuracy, however, it is costlier and time-consuming. Therefore, it should be a compromise between the required accuracy and time/cost. Next, we run the robot from one end to the other end, collecting the RSSI signal patterns for each tag along the pipe that maps to the robot's location to generate the measurement model. The robot's accurate location (ground truth) was determined using the laser distance measurement unit. For the test data, the robot was deployed 10 times inside the 5m pipe placing previously measured UHF-RFID tags approximately 1 meter apart from each other, and in each deployment, we attached new sets of tags (in a total of 50 different tags were used) that mimics approximately a 50m long UHF-RFID pipe scan (Fig. 3). RSSI data relating to the first 10 UHF-RFID tags is shown in Fig. 4.

The robot is deployed in the pipe section, where the UHF-RFID locations are unknown. Fig. 5 shows an example result of the RSSI signal mapping for a given UHF-RFID tag and for a given antenna. The top graph shows the measurement model signal that maps the laser distance reading to the signal pattern. The middle graph contains the received signal data (note the x-axis scale differences) that needs to be aligned with the measurement model to estimate the travel distance. The bottommost graph shows the results of mapping the received signal to the measurement model signal, which leads to correlating the data points with distance values.

C. In-pipe Robot Localization and UHF-RFID Mapping

Robot localization accuracy calculated based on laser system is shown in Fig. 6. Fig. 7 shows the mean error graph

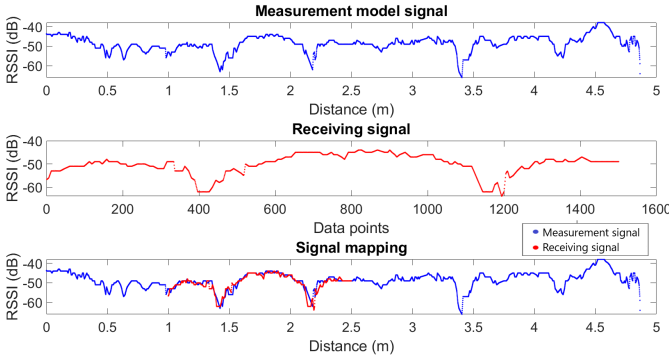

Fig. 5: Signal cross-correlation mapping between the measurement signal and the received signal.

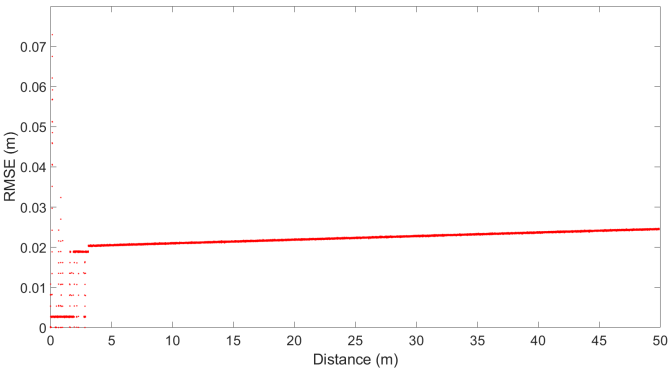

Fig. 6: In-pipe robot SLAM performance (robot speed at 0.1m/s). The comparison of the SLAM location with respect to the groundtruth location.

where it has an initial slightly poor performance. It is due to a lack of received UHF-RFID signal data points, however, it improved significantly within the first 3 meters. This can be alleviated by adding several RFIDs at the beginning of the pipe section.

It is to be noted that the currently used hardware can only receive data at an approximate 50Hz rate. Therefore, the density and the quality of the received signal data depend on the robot's speed. Higher robot speeds lead to larger errors as shown in Fig. 8. Fig. 9 shows the UHF-RFID signals received from the two antennas while travelling inside the pipelines.

D. Performance Evaluation

Performance of the proposed algorithm was compared with industry standard, commonly used encoder odometry based robot localization (OD) and also with the Gaussian process combined particle filter based two antenna model localization method (GPPF2) we have proposed in our preliminary research work [31], [32].

As in Fig. 10, the GPPF2 shows higher accuracy, however it requires the exact locations of the RFID tags to be known. The proposed SLAM approach managed to achieve a slightly lower accuracy without any knowledge of the RFID tag distribution.

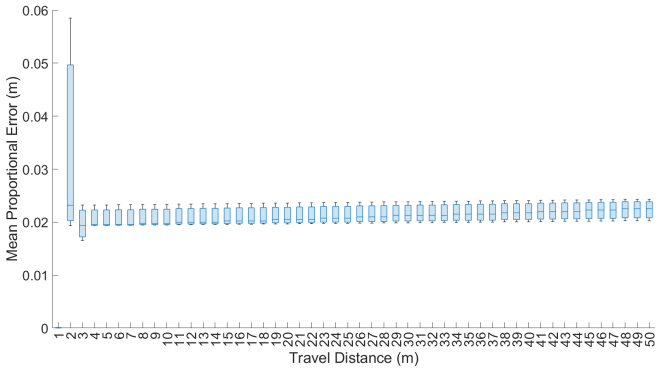

Fig. 7: The Whiskers plot graph consists of 20 sets of trials with random movement noise.

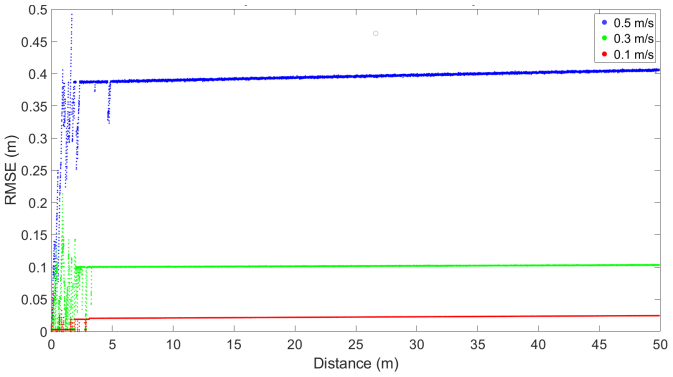

Fig. 8: In-pipe SLAM performance at different speeds of the robot.

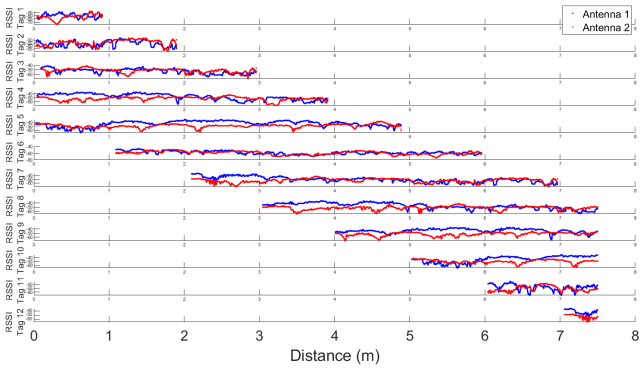

Fig. 9: UHF-RFID sensor tag signal mapping results at 7.5m.

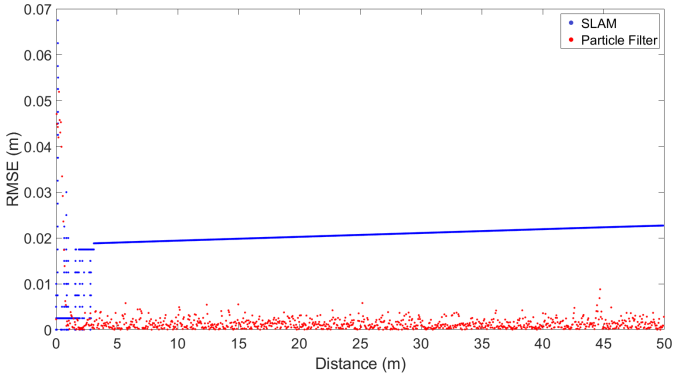

Fig. 10: Particle filter vs. SLAM performance comparison.

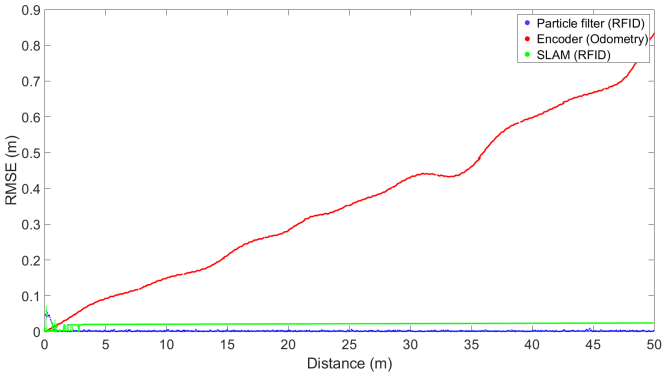

Fig. 11: Particle filter vs. SLAM performance vs. encoder odometry comparison.

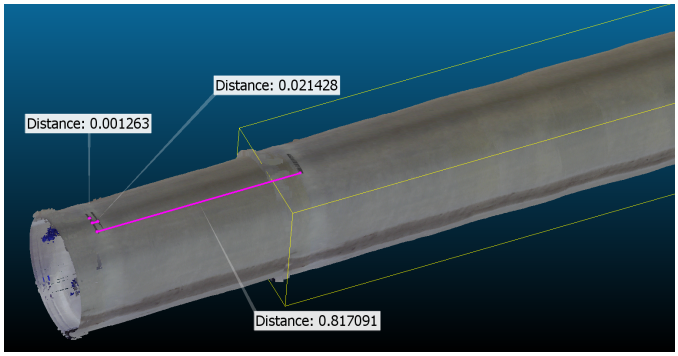

Fig. 12: Laser profile localization evaluation - UHF-RFID vs. Encoder.

Fig. 11 shows the comparison between the proposed SLAM, GPPF2 and OD. It shows error caused by the accumulated drift of the odometry based localization.

Fig. 12 shows the end results of a 50m pipe deployment. A physical mark on the crown of the pipe has been used to correlate the localization errors. It is clearly seen that the OD localization is 0.817 meters away from the ground truth. The GPPF2 with known RFID locations perfectly aligned with the ground truth with an insignificant (0.001m) deviation. The proposed SLAM localization aligns within 0.021m. Therefore, the most practically effective solution is the proposed UHF-RFID SLAM.

Table I summarizes the comparison results. The localization methods proposed in this journal show competitive accuracy compared with results for other methods reported in the literature. Two typical conventional localization methods [18], [19] show around 31cm and 27cm accuracy; two methods employing two UHF-RFID antennas in recent studies [20], [21] for outdoor and indoor localization show around 50cm and 6cm accuracy; and an in-pipe localization method proposed by [28] shows approximately 25cm accuracy. The UHF-RFID SLAM proposed in this journal exhibits superior accuracy of 2.5cm inside pipelines.

VI. Conclusion and Future Work

This article presents the development of battery-free UHF-RFID sensors based SLAM for in-pipe robotic localization.

Method	Position error Mean (mm)	Position error Std. dev. (mm)
A sparse RFID tag distribution method in [19]	271	113
Motion-continuity property of the differential-driving mobile robot method in [18]	310	139
Bayesian filter and a variable power RFID model proposed in [20]	500	200
Localization combining phase difference of double antennas proposed in [21]	59	36
Localization approach using IMU, gyro, and the leak sensors proposed in [28]	250	Not Given
Encoder based method	833	214
Proposed GP based PF method in [34]	1.8	1.62
Proposed SLAM method	23.3	3.8

TABLE I: Performance comparison with existing localization methods.

A mobile robotic prototype which is capable of navigating in pipes with diameters ranging from 450mm to 650mm was developed. A signal cross-correlation mapping technique in combination with a customized simultaneous localization and mapping algorithm was developed to estimate the location of the robot. It was tested up to a 50m long pipeline using a sample pipe taken from the Sydney water underground pipe network.

The findings demonstrated that the proposed approach is capable of localizing the robot with an accuracy of approximately 2.5cm while using UHF-RFID tag locations that are unknown. The effect of robot traverse speed on localization accuracy was investigated using a series of experiments. According to the experimental findings, faster speeds result in more errors since the number of data points received is reduced as a consequence. One way to improve the accuracy is to deploy RFIDs at shorter intervals

Larger pipelines like the ones reported in this study are generally consisting of straight line sections. Hence the localization is mostly one-dimensional and accurate enough for the application. Pipes are made of metallic cast iron and act as a Faraday cage, hence Electromagnetic interference to RFID signals is negligible.

The initial cost estimate for a robotic system with an RFID dual antenna system costs $1250. For the RFID tags, it costs approximately $4 per meter. The encoder-based systems require neither the antenna cost which is $100 each nor the RFID tags cost, while it cannot produce the accuracy required for the application. Cost may be a factor to consider in making decisions about using the system. However, considering the millions of dollar budget allocated for condition assessment of pipes, this is a reasonable cost-effective solution. When compared with current literature and the most extensively used industry standard, encoder-based localization strategy, the proposed method outperformed in terms of accuracy.

In the future, we intend to test the technology in longer pipe sections under a variety of environmental circumstances when COVID constraints have been lifted. The research may be further developed in order to produce a more generalized signal model for enhancing the deployment efficacy of UHF-RFID tags by studying the signal repeatability characteristics of the UHF-RFID tags themselves.

ACKNOWLEDGMENT

This work was supported by the University of Technology Sydney (UTS) through the Faculty of Engineering and Information Technology (FEIT) Tech Lab Blue Sky Research Grant.

REFERENCES

[1] K. Thiyagarajan, S. Kodagoda, R. Ranasinghe, G. Iori, and D. Vitanage, "Robust Sensor Suite Combined with Predictive Analytics Enabled Anomaly Detection Model for Smart Monitoring of Concrete Sewer Pipe Surface Moisture Conditions," *IEEE Sensors Journal*, vol. 20, no. 15, pp. 8232–8243, 2020.

[2] N. Ulapane, K. Thiyagarajan, J. Miro, and S. Kodagoda, "Surface Representation of Pulsed Eddy Current Sensor Signals for Improved Ferromagnetic Material Thickness Quantification," *IEEE Sensors Journal*, vol. 21, no. 4, pp. 5413–5422, 2021.

[3] K. Thiyagarajan, S. Kodagoda, R. Ranasinghe, D. Vitanage, and G. Iori, "Robust sensing suite for measuring temporal dynamics of surface temperature in sewers," *Scientific Reports*, vol. 8, no. 1, p. 16020, 2018.

[4] K. Thiyagarajan, S. Kodagoda, L. V. Nguyen, and R. Ranasinghe, "Sensor Failure Detection and Faulty Data Accommodation Approach for Instrumented Wastewater Infrastructures," *IEEE Access*, vol. 6, pp. 56 562–56 574, 2018.

[5] J. C. Matthews, A. Selvakumar, and W. Condit, "Demonstration and evaluation of an innovative water main rehabilitation technology: Cured-in-Place Pipe (CIPP) lining," *Water Practice and Technology*, vol. 7, no. 2, Jun. 2012. [Online]. Available: https://doi.org/10.2166/wpt.2012.028

[6] R. Azoor, B. Shannon, G. Fu, R. Deo, and J. Kodikara, "Performance of field-aged polymeric spray lining for water pipe rehabilitation," *Tunnelling and Underground Space Technology*, vol. 116, p. 104116, Oct. 2021. [Online]. Available: https://doi.org/10.1016/j.tust.2021.104116

[7] J. V. Miro, N. Ulapane, L. Shi, D. Hunt, and M. Behrens, "Robotic pipeline wall thickness evaluation for dense nondestructive testing inspection," *Journal of Field Robotics*, vol. 35, no. 8, pp. 1293–1310, Nov. 2018.

[8] L. Nguyen and J. V. Miro, "An Efficient 3-D Model for Remaining Wall Thicknesses of Cast Iron Pipes in Nondestructive Testing," *IEEE Sensors Letters*, vol. 4, no. 7, pp. 1–4, Jul. 2020. [Online]. Available: https://doi.org/10.1109/lsens.2020.2999330

[9] S. Kodagoda and K. Thiyagarajan, "Performance Monitoring of Liners: Parameter Identification," Oct 2018. [Online]. Available: https://www.waterportal.com.au/smartlinings/images/Deliverables/31_UTS_Literature_Review_FINAL.pdf

[10] D. Vasilikis and S. Karamanos, "Mechanical behavior and wrinkling of lined pipes," *International Journal of Solids and Structures*, vol. 49, p. 3432–3446, 11 2012.

[11] D. Sharma, M. Rawat, J. Sharma, S. Ahuja, A. Chandra, S. Barman, and R. Arya, *Polymer Coatings Technology and Applications: Polymer Coating Mehods*. CRC Press, 01 2021.

[12] A. Gunatilake, L. Piyathilaka, A. Tran, V. K. Vishwanathan, K. Thiyagarajan, and S. Kodagoda, "Stereo Vision Combined With Laser Profiling for Mapping of Pipeline Internal Defects," *IEEE Sensors Journal*, vol. 21, no. 10, pp. 11 926–11 934, 2021. [Online]. Available: https://doi.org/10.1109/JSEN.2020.3040396

[13] A. Gunatilake, L. Piyathilaka, S. Kodagoda, S. Barclay, and D. Vitanage, "Real-Time 3D Profiling with RGB-D Mapping in Pipelines Using Stereo Camera Vision and Structured IR Laser Ring," in *2019 14th IEEE Conference on Industrial Electronics and Applications (ICIEA)*, 2019, pp. 916–921.
[14] E. Giannelos, E. Andrianakis, K. Skyvalakis, A. G. Dimitriou, and A. Bletsas, "Robust RFID Localization in Multipath with Phase-Based Particle Filtering and a Mobile Robot," *IEEE Journal of Radio Frequency Identification*, pp. 1–1, 2021.
[15] E. DiGiampaolo and F. Martinelli, "A Robotic System for Localization of Passive UHF-RFID Tagged Objects on Shelves," *IEEE Sensors Journal*, vol. 18, no. 20, pp. 8558–8568, 2018.
[16] A. Tzitzis, S. Megalou, S. Siachalou, T. G. Emmanouil, A. Kehagias, T. V. Yioultsis, and A. G. Dimitriou, "Localization of RFID Tags by a Moving Robot, via Phase Unwrapping and Non-Linear Optimization," *IEEE Journal of Radio Frequency Identification*, vol. 3, no. 4, pp. 216–226, 2019.
[17] F. Bernardini, A. Buffi, D. Fontanelli, D. Macii, V. Magnago, M. Marracci, A. Motroni, P. Nepa, and B. Tellini, "Robot-Based Indoor Positioning of UHF-RFID Tags: The SAR Method With Multiple Trajectories," *IEEE Transactions on Instrumentation and Measurement*, vol. 70, pp. 1–15, 2021.
[18] S. Han, H. Lim, and J. Lee, "An Efficient Localization Scheme for a Differential-Driving Mobile Robot Based on RFID System," *IEEE Transactions on Industrial Electronics*, vol. 54, no. 6, pp. 3362–3369, 2007.
[19] P. Yang, W. Wu, M. Moniri, and C. C. Chibelushi, "Efficient Object Localization Using Sparsely Distributed Passive RFID Tags," *IEEE Transactions on Industrial Electronics*, vol. 60, no. 12, pp. 5914–5924, 2013.
[20] J. Zhang, Y. Lyu, J. Patton, S. C. G. Periaswamy, and T. Roppel, "BFVP: A Probabilistic UHF RFID Tag Localization Algorithm Using Bayesian Filter and a Variable Power RFID Model," *IEEE Transactions on Industrial Electronics*, vol. 65, no. 10, pp. 8250–8259, 2018.
[21] B. Tao, H. Wu, Z. Gong, Z. Yin, and H. Ding, "An RFID-Based Mobile Robot Localization Method Combining Phase Difference and Readability," *IEEE Transactions on Automation Science and Engineering*, vol. 18, no. 3, pp. 1406–1416, 2021.
[22] S. R. Rusu, M. J. D. Hayes, and J. A. Marshall, "Localization in large-scale underground environments with RFID," in *2011 24th Canadian Conference on Electrical and Computer Engineering(CCECE)*, 2011, pp. 001 140–001 143.
[23] C. Li, L. Mo, and D. Zhang, "Review on UHF RFID Localization Methods," *IEEE Journal of Radio Frequency Identification*, vol. 3, no. 4, pp. 205–215, 2019.
[24] E. DiGiampaolo and F. Martinelli, "A restarting paradigm for a Range-Only SLAM algorithm using the phase of passive UHF-RFID signals," in *2019 IEEE International Conference on RFID Technology and Applications (RFID-TA)*, 2019, pp. 279–284.
[25] F. Martinelli, "Robot Localization Using the Phase of Passive UHF-RFID Signals Under Uncertain Tag Coordinates," *Journal of Intelligent & Robotic Systems*, vol. 82, pp. 577–593, 2016.
[26] J. Virtanen, L. Ukkonen, T. Björninen, L. Sydänheimo, and A. Z. Elsherbeni, "Temperature sensor tag for passive UHF RFID systems," in *2011 IEEE Sensors Applications Symposium*, 2011, pp. 312–317.
[27] E. M. Amin, M. S. Bhuiyan, N. C. Karmakar, and B. Winther-Jensen, "Development of a Low Cost Printable Chipless RFID Humidity Sensor," *IEEE Sensors Journal*, vol. 14, no. 1, pp. 140–149, 2014.
[28] Y. Wu, E. Mittmann, C. Winston, and K. Youcef-Toumi, "A Practical Minimalism Approach to In-pipe Robot Localization," in *2019 American Control Conference (ACC)*, 2019, pp. 3180–3187.
[29] A. Buffi, P. Nepa, and R. Cioni, "SARFID on drone: Drone-based UHF-RFID tag localization," in *2017 IEEE International Conference on RFID Technology Application (RFID-TA)*, 2017, pp. 40–44.
[30] F. Martinelli, "A Robot Localization System Combining RSSI and Phase Shift in UHF-RFID Signals," *IEEE Transactions on Control Systems Technology*, vol. 23, no. 5, pp. 1782–1796, 2015.
[31] A. Gunatilake, M. Galea, K. Thiyagarajan, S. Kodagoda, L. Piyathilaka, and P. Darji, "Using UHF-RFID Signals for Robot Localization Inside Pipelines," in *2021 IEEE 16th Conference on Industrial Electronics and Applications (ICIEA)*, 2021, pp. 1109–1114.
[32] A. Gunatilake, K. Thiyagarajan, and S. Kodagoda, "Evaluation of Battery-free UHF-RFID Sensor Wireless Signals for In-pipe Robotic Applications," in *2021 IEEE SENSORS*, 2021, pp. 1–4.
[33] J. Zhang, Y. Lyu, J. Patton, S. C. G. Periaswamy, and T. Roppel, "BFVP: A Probabilistic UHF RFID Tag Localization Algorithm Using Bayesian Filter and a Variable Power RFID Model," *IEEE Transactions on Industrial Electronics*, vol. 65, no. 10, pp. 8250–8259, 2018.
[34] A. Gunatilake, S. Kodagoda, and K. Thiyagarajan, "A Novel UHF-RFID Dual Antenna Signals Combined With Gaussian Process and Particle Filter for In-Pipe Robot Localization," *IEEE Robotics and Automation Letters*, vol. 7, no. 3, pp. 6005–6011, 2022.
[35] S. Thrun, W. Burgard, D. Fox, and R. Arkin, *Probabilistic Robotics*, ser. Intelligent Robotics and Autonomous Agents series. MIT Press, 2005. [Online]. Available: https://books.google.com.au/books?id=2Zn6AQAAQBAJ
[36] W. Lin, J. Hu, H. Xu, C. Ye, X. Ye, and Z. Li, "Graph-based SLAM in indoor environment using corner feature from laser sensor," in *2017 32nd Youth Academic Annual Conference of Chinese Association of Automation (YAC)*, 2017, pp. 1211–1216.
[37] H. Durrant-Whyte and T. Bailey, "Simultaneous localization and mapping: part I," *IEEE Robotics Automation Magazine*, vol. 13, no. 2, pp. 99–110, 2006.

Amal Gunatilake (Member, IEEE) received the diploma in electrical and electronic engineering from the Arthur C. Clark Institute for Modern Technologies, Sri Lanka, in 2007, the B.Eng. (Hons.) degree in software engineering from the University of Westminster, UK, in 2013, and the Ph.D. degree in robotics from the University of Technology Sydney, Sydney, Australia, in 2021.

He has worked over 5 years in the open-source software engineering industry as a Senior Software Engineer to research and develop IoT software products. He was in the Executive Committee of the IEEE Sensor Council New South Wales chapter, Australia in 2020.

Dr. Amal currently works as a Research Fellow at UTS Robotics Institute, University of Technology Sydney, Australia. His current research interests include robotic sensing and perception, SLAM using unconventional sensors, machine learning and infrastructure robotics.

Sarath Kodagoda (Member, IEEE) received the B.Sc. Eng. (Hons.) degree in electrical engineering from the University of Moratuwa, Sri Lanka, in 1995, and the M.Eng. and Ph.D. degrees in robotics from Nanyang Technological University, Singapore, in 2000 and 2004, respectively.

He is currently a Professor and Director of the UTS Robotics Institute, the Founder of the iPipes Lab, and a Program Coordinator of the Mechanical and Mechatronics degree at the University of Technology Sydney, Australia. He is also the President of the Australian Robotics and Automation Association. His current research interests include infrastructure robotics, sensors and perception, machine learning and human-robot interaction.

Prof. Kodagoda's works in in-pipe sensing and robotics has won several awards including the 2020 National Research Innovation Award from the Australian Water Association.

Karthick Thiyagarajan (Member, IEEE) received the B.E. degree in electronics and instrumentation engineering from the Anna University, Chennai, India, in 2011, the M.Sc. degree in mechatronics from the University of Newcastle Upon Tyne, Newcastle Upon Tyne, U.K., in 2013, and the Ph.D. degree specializing in smart sensing from the University of Technology Sydney, Sydney, Australia, in 2018.

He is currently a Research Fellow and Smart Sensing Technologies Research Lead with the iPipes Lab, UTS Robotics Institute, University of Technology Sydney, Australia. His current research interests are in the development of intelligent sensing and perception technologies for infrastructure robotics, field robotics, assistive robotics, human-robot interaction and environmental monitoring.

Dr. Thiyagarajan is also serving as a Secretary for the IEEE Sensors Council New South Wales Chapter, Australia, in 2022, and Executive Committee Member of the IEEE Sensors Council Young Professionals and Publicity Committee in 2022.